Published in *Applied Catalysis A: General, vol. 349, pp. 189-197 (2008)*
http://dx.doi.org/10.1016/j.apcata.2008.07.038

PHOTOCATALYTIC OXIDATION OF AROMATIC ALCOHOLS TO ALDEHYDES IN AQUEOUS SUSPENSION OF HOME PREPARED TITANIUM DIOXIDE
2. INTRINSIC AND SURFACE FEATURES OF CATALYSTS

Vincenzo Augugliaro,[a*] Horst Kisch,[b] Vittorio Loddo,[a] María José López-Muñoz,[c] Carlos Márquez-Álvarez,[d] Giovanni Palmisano,[a] Leonardo Palmisano,[a*] Francesco Parrino,[b] Sedat Yurdakal[a,e]

[a] "Schiavello-Grillone" Photocatalysis Group, Dipartimento di Ingegneria Chimica dei Processi e dei Materiali, Università degli Studi di Palermo, Viale delle Scienze, 90128 Palermo, Italy

[b] Institute of Inorganic Chemistry, University of Erlangen-Nürnberg, Egerlandstrasse 1, D-91058 Erlangen, Germany

[c] Department of Chemical and Environmental Technology, ESCET, Rey Juan Carlos University, C/Tulipán s/n, 28933 Móstoles, Madrid, Spain

[d] Instituto de Catálisis y Petroleoquímica, CSIC, C/Marie Curie 2, 28049 Cantoblanco, Madrid, Spain

[e] Kimya Bölümü, Fen Fakültesi, Anadolu Üniversitesi, Yunus Emre Kampüsü, 26470 Eskişehir, Turkey

Dedicated to the friendship between Pablo Neruda and Nazım Hikmet

[*]Corresponding authors
E-mail: augugliaro@dicpm.unipa.it, palmisano@dicpm.unipa.it

KEYWORDS: photocatalysis, TiO_2, *in situ* ATR-FTIR analysis, aromatic alcohols, selective oxidation, aliphatic alcohol

ABSTRACT

As reported in an accompanying contribution [1], home-prepared (HP) TiO_2 powders were used for carrying out the photocatalytic oxidation of benzyl alcohol (BA) in water. The addition of small amounts of ethanol decreases the oxidation rate of BA but it enhances the selectivity for aldehyde formation. The catalysts textural characterization, carried out with XRD, SEM observations, BET surface area and porosity measurements, has been elsewhere reported [1]. In this paper some intrinsic electronic properties were investigated by Diffuse Reflectance Spectroscopy and quasi-Fermi Level measurements. The values of band gap, valence band and conduction band edges are almost identical for all the HP samples in which anatase phase is predominant, whereas appreciable differences can be noticed for an HP sample containing high amount of rutile phase. A comparative ATR-FTIR study of the HP catalyst showing the highest selectivity and the commercial titania showing the highest activity towards BA oxidation (Degussa P25 TiO_2) was carried out. The ATR-FTIR results indicate that HP and Degussa P25 surfaces show a very dissimilar hydrophilicity and different ability for adsorbing the organic compounds deriving from benzyl alcohol photocatalytic oxidation. Results show moreover that the improved selectivity to aldehyde by adding ethanol is due to a competition between the substrate and the ethanol for adsorption on reactive sites.

1. INTRODUCTION

The accompanying contribution [1] of this paper has been devoted to study the selective oxidation of benzyl alcohol (BA) to benzaldehyde (BAD) in water by using irradiated TiO_2 catalysts. The photoreactivity runs were carried out with aqueous suspensions of different home prepared (HP) TiO_2 specimens and of a commercial TiO_2 catalyst (Degussa P25). The performances of catalysts were compared in terms of BA oxidation rate and selectivity towards BAD production. The HP catalysts exhibited reaction rates always lower than that of the commercial one but selectivity values about four times higher. The addition to the HP catalyst suspension of ethanol decreases the overall oxidation rate of BA but it determines a significant improvement of the photoprocess selectivity towards aldehyde. The selectivity enhancement by ethanol seems to be specific of HP catalysts, this effect being negligible with Degussa P25.

The results of HP catalysts textural characterization, carried out with XRD, SEM observations, BET surface area and porosity measurements, are elsewhere reported [1]. The main aim of this investigation was that of finding likely explanations for the different photoactivity shown by HP and commercial catalysts. In order to reach this goal, bulk and surface properties have been investigated. For the first ones some intrinsic electronic features of catalysts were investigated by Diffuse Reflectance Spectroscopy and quasi-Fermi Level measurements; for the second ones *in situ* attenuated total reflection Fourier transform infrared (ATR-FTIR) spectroscopy has been used. The ATR-FTIR study has been focused on the comparison of the HP catalyst showing the highest selectivity and the Degussa P25 TiO_2 sample, which exhibits the highest activity for the BA photocatalytic oxidation. The features of the interaction of BA with the catalyst surface, the identification of the species adsorbed on catalyst upon photooxidation of BA and the effect of water and ethanol on the overall process were investigated. The water adsorption capability of both catalysts was also investigated by thermogravimetric analysis.

2. EXPERIMENTAL

2.1 Catalysts preparation and characterization

The preparation method has been reported elsewhere [2]. The precursor solution was obtained by adding 5 mL of $TiCl_4$ drop by drop into a 200 mL beaker containing 50 mL of water. During the addition, that lasted 5 min, the solution was magnetically stirred by a cylindrical bar (length, 3 cm; diameter, 0.5 cm) at 600 rpm. After that the beaker was closed and mixing was prolonged for 12 h at room temperature, eventually obtaining a clear solution. This solution was transferred to a round-bottom flask fitted with a Graham condenser. The flask was heated in boiling water for 0.5, 2, 4, 6 and 8 h, obtaining a white suspension at the end of each treatment. The suspension was then dried at 323 K by means of a rotovapor machine (model Buchi Rotovapor M) working at 50 rpm, in order to obtain the final powdered catalysts. The HP powders were washed with distilled water and centrifuged several times until the chloride ion concentration in the washing water reached a negligible value, as checked by $AgNO_3$ test. Hereafter the home prepared catalysts are referred to as "HPx" in which the x figure indicates the boiling time of the precursor, expressed in hours.

Diffuse reflectance spectra of the solids were obtained using a UV-Vis spectrophotometer (Shimadzu, UV-2401PC). Samples were spread onto $BaSO_4$ plates; the background reflectance of $BaSO_4$ was measured before. Reflectance was converted by the instrument software to $F(R_\infty)$ values according to the Kubelka-Munk theory [3].

Thermogravimetric analyses were performed by using a Netzch equipment (model STA 409). The heating rate was 10 °C/min in static air and the powder amount, put in open Pt crucible, was 190 mg for all the samples.

All the chemicals used for preparation and characterization studies were purchased from Sigma Aldrich with purity > 99 %.

2.2 Photoelectrochemical measurements

According to the literature [4] 50 mg of catalyst and 10 mg of methyl viologen dichloride were suspended in a 100 mL two-necked flask in 50 mL of 0.1 M KNO_3. A platinum flag and Ag/AgCl served as working and reference electrodes, respectively. A pH-meter allowed to follow the proton concentration; HNO_3 (0.1M) and NaOH were used to adjust the pH value. The

suspension was magnetically stirred and flushed with dinitrogen throughout the experiment carried out at room temperature. In general the starting suspension had pH 2.5. In order to check the influence of ethanol on the flat band potential, 5 ml of ethanol (Merck, 99.9%) were added into the suspension and the same procedure was carried out. Irradiation was performed with a 150 W xenon arc lamp (OSRAM XBO, I_0 (300-400 nm) = $1.4 \cdot 10^{-6}$ Einstein$\cdot s^{-1} \cdot cm^{-2}$) installed in a light-condensing lamp housing (PTI, A1010S) on an optical train. The flask was mounted at a distance of 30 cm from the lamp.

2.3 *In situ* ATR-FTIR measurements

Infrared spectra of thin films of the photocatalysts were recorded using a Thermo Nicolet Nexus FTIR spectrometer equipped with a liquid nitrogen-cooled MCT detector and a SensIR Technologies DurasamplIR 9-reflection horizontal ATR accessory (4 mm diameter diamond-faced ZnSe prism). Titania samples grounded in an agate mortar were suspended in Milli-Q deionized water (25 mg solid in 25 mL water) and sonicated for 20 min (Elma Transsonic T470/H ultrasonic cleaning unit). Thin films were prepared by dropping 50 μL of the suspension onto the ATR crystal and then allowing the solvent to evaporate. The procedure was repeated twice to obtain thin films containing ca. 100 μg TiO_2. A 100 mL volume glass flow cell was attached to the ATR plate through an o-ring sealed connection and the thin film was dried at room temperature for several minutes in a stream of synthetic air (Air Liquide, Alphagaz Air 1). Adsorption of water, ethanol (Panreac, 99.5%) and benzyl alcohol (Sigma-Aldrich, purity > 99%) vapours on the dried TiO_2 thin films was carried out at room temperature under static conditions by introducing 0.2 mL of each liquid adsorbate inside the closed glass cell previously purged with synthetic air. After adsorption in the dark for around 1 h, UV irradiation of the photocatalyst films in contact with the water/alcohol-saturated air atmosphere was performed using an 80 W mercury vapour lamp (OSRAM HQL de luxe MBF-U). The light was filtered by passing through a Pyrex vessel containing a 0.1 M $CuSO_4$ aqueous solution. Time-resolved FTIR spectra in the 4000-900 cm^{-1} wavenumber range, with a resolution of 4 cm^{-1}, were recorded along with the adsorption and irradiation steps at room temperature. Each spectrum was obtained by averaging 10 scans accumulated in 4 seconds. Happ-Genzel apodization function was applied. The spectra were referenced against the spectrum of the dried TiO_2 thin film.

3. RESULTS AND DISCUSSION

3.1 Catalysts characterization

Figure 1 exhibits the transformed diffuse reflectance spectra of two HP catalysts, i.e. HP0.5 and HP8; the plots report the values of $[F(R_\infty)\cdot E]^{0.5}$, the modified Kubelka-Munk function, versus E, the energy of exciting light. The weak low-energy shoulder may correspond to the presence of rutile phase; its intensity, proportional to the rutile amount, increases by increasing the boiling time. The corresponding band gap energies of all the used HP and commercial catalysts were obtained from plots like those reported in Fig. 1, assuming that the solids are indirect crystalline semiconductors [5]. The band gap values are reported in Table 1; these values are quite similar for predominantly anatase phase catalysts.

Thermogravimetric and time derivative curves of Degussa P25 and HP0.5 samples are shown and compared in Fig. 2. Degussa P25 is stable up to 800 ºC and it shows only 1 % weight change due to the occurrence of a release of adsorbed moisture below 100 ºC. For HP0.5 sample the TG curve shows that it contains a significant amount of physically adsorbed water, about 10 % weight; in fact the evaporation of bound water becomes significant at about 80 ºC, and the highest rate of mass losses is reached at around 140 ºC. It is remarkable that the loss of water continues up to 350 ºC thus indicating that the energy of interaction between water molecules and HP0.5 surface covers a wide range.

The quasi-Fermi level of electrons, E_{fb}, was determined according to literature [4] by measuring the photovoltage in the presence of methylviologen, MV, as a function of pH value. Figure 3 reports the measurements obtained with all HP catalysts. Upon increasing the pH value, a blue color is developed when approaching the inflection point, pH_0, due to formation of the methylviologen radical cation. A lower pH_0 value corresponds to a more negative quasi-Fermi level. From pH_0 value of the corresponding titration curve (see Fig. 3), the quasi-Fermi level at pH 7 can be calculated via eqn. 1:

$$E_{fb} = E^0_{MV^{2+}/MV^{+\cdot}} + k\,(pH_0 - pH) \qquad (1)$$

where $E^0_{MV^{2+}/MV^{+\cdot}}$ is the redox potential of the $MV^{2+}/MV^{+\cdot}$ couple and k is assumed equal to 0.059 V. The E_{fb} values of all catalysts are reported in Table 1; it may be noted that the position of the quasi Fermi level for Degussa P25 and HP0.5 to HP6 samples is about the same (-0.55 and -0.52 V, respectively) indicating that interfacial electron transfer to methylviologen proceeds from the anatase conduction band. However, in the case of HP8 this value is –0.37 V, which is characteristic for rutile type TiO_2 and indicates that reduction of methylviologen occurs via electrons trapped at the rutile conduction band. By assuming that the difference between the quasi-Fermi level potential and conduction band edge is negligible, the valence band edge values can be obtained by addition of the band gap energy. HP0.5, HP2, and HP4 band edge is located at 2.84 V, whereas it is shifted to 2.74 V for HP6, which contains a significant amount of rutile, and for HP8, nearly pure rutile.

These results indicate that the photoelectrochemical features of anatase and anatase-rutile catalysts are very similar. On this basis it is likely that these properties play a minor role in determining the differences of reactivity and selectivity shown by these samples [1].

In the presence of 10 % vol of ethanol the flatband potential of HP0.5 was shifted cathodically by about 0.06 V (see Fig. 4) while the shift was about 0.09 V in the case of P25. Similar shifts had been reported in the literature [6] when the flatband potential of titania was measured in non-diluted methanol. From these results one can conclude that in aqueous ethanol solution the reductive power of the reactive electron in anatase powders is much higher than in pure water.

3.2 ATR-FTIR analysis

3.2.1. Adsorption of water and benzyl alcohol on HP0.5

Figure 5 displays the in situ ATR-FTIR spectra acquired when exposing HP0.5 in an atmosphere of synthetic air saturated with BA and water. The great enhancement over time in the intensity of the absorption band centred at 1640 cm^{-1} due to the bending vibration mode of adsorbed molecular water indicates a remarkable hydrophilicity of the HP0.5 surface. The clear tailing of the δ(HOH) vibration band towards low frequencies may be indicative of different adsorption sites for molecular water.

Bands growing in at 1497, 1455, 1369, 1208, 1079, 1035, 1018 and 1006 cm^{-1} are mainly the same as those in pure BA (see Fig. 5). At high frequencies, a broad and strong absorption showing two maxima at ca. 3400 cm^{-1} and 3240 cm^{-1} is detected indicating the presence of hydrogen-bonded perturbed OH groups and water. Two weak bands superimposed to this broad absorption appear at 3066 and 3033 cm^{-1}, which are ascribed to the C-H stretching vibrations of the aromatic ring of the alcohol. The bands at 1497 and 1455 cm^{-1} can be readily assigned to skeletal vibrations of the aromatic ring and the band centred at 1208 cm^{-1} to the C-C stretching vibration. The band centred at 1369 cm^{-1} can be attributed to the O-H in-plane deformation mode of the alcohol [7]. The presence of this band is indicative of non-dissociative adsorption of BA on the HP0.5 surface. According to these FTIR spectra, molecularly adsorbed BA appears to be the predominant surface organic species formed.

It is usually reported that adsorption of alcohols on metal oxide surfaces leads to the formation of alcoholate species. However, in the present study, the identification of adsorbed benzolate on HP0.5 sample is not straightforward. To the best of our knowledge, infrared spectra of benzolate species on hydroxylated titania have not been reported up-to-date. Moreover, the close wavenumber values usually observed for the different vibration bands of alcohols and their corresponding alcoholate species hinders an unequivocal assignment. In the present case, a clear indication of benzolate formation could be obtained from the analysis of the evolution of the C-C and C-O stretching modes region (bands at 1035, 1018 and 1006 cm^{-1}), as formation of alcoholate species should be accompanied by a significant blue shift of the alcohol C-O stretching band. As adsorption of BA progresses, a band centred at 1041 cm^{-1} grows superimposed to the band located at 1035 cm^{-1}. This shift does not seem to be large enough to definitively justify the formation of benzyl alcoholate species but in any case it is indicative of the existence of different adsorption sites on the HP0.5 surface or different ways of interaction between BA and the sample surface.

Figure 6 displays the time evolution of the amounts of water and BA adsorbed on HP0.5; those amounts are plotted as the integrated absorbance of selected IR bands. It can be observed that in the first 10 minutes the amounts of both adsorbed water and BA continuously increase. However, the quantity of adsorbed alcohol reaches a maximum and then it monotonously decreases with time, while the amount of adsorbed water continuously increases, thus indicating

that water favourably competes with BA for adsorption determining a partial displacement of BA from the TiO_2 surface.

3.2.2. Adsorption of water and benzyl alcohol on commercial TiO_2

The adsorption of BA and water on Degussa P25, following a similar experimental procedure, gives rise to spectra that show remarkable differences with respect to HP0.5 sample (see Fig. 7). It is worth to note that the intensity of the absorption band centred at 1645 cm^{-1} due to the δ(HOH) vibration of molecularly adsorbed water appears for Degussa P25 with much lesser intensity than for HP0.5 sample (note that the integrated absorbance scale for water in Fig. 6 is 10 times larger for this sample), thus indicating the substantially lower hydrophilicity of the Degussa P25 surface. This finding is also in accord with TG measurements (see Fig. 2). Adsorption of BA molecules with scarce modifications is demonstrated by the presence of absorption bands at 1498, 1454, 1372, 1208, 1078 and 1037 cm^{-1}. The time evolution of the integrated absorbance of IR bands at 1208 and 1640 cm^{-1} (see Fig. 6) shows that the amounts of BA adsorbed on HP0.5 and Degussa P25 are comparable; however the BA amount per unit surface area is ca. 5 times higher in Degussa P25 than in HP0.5. Figure 6 also shows that water is able to displace part of adsorbed BA but, owing to the much lesser amount of water adsorbed on Degussa P25, the displacement of the alcohol is slower than in HP0.5 sample.

Besides the above mentioned bands ascribable to the adsorbed alcohol, a group of absorptions (not observed with HP0.5 sample) at 1413, 1340 and 1156 cm^{-1} are also detected in the spectra displayed in Fig. 7. The band centred at 1156 cm^{-1} might be ascribed to a C-O stretching vibration; its blue shift with respect to the molecular alcohol is, in contrast with that previously discussed for HP0.5, large enough to indicate the formation of adsorbed benzolate species. On this basis, it may be hypothesized the presence of two distinct adsorption sites for BA on the Degussa P25 surface. Additionally, weak features are initially formed at 1705, 1602 and 1584 cm^{-1}, although as adsorption progresses they are obscured by the strong water absorption at 1645 cm^{-1}. The frequency value of 1705 cm^{-1} points out to the presence of carbonyl group. In the high-frequency region, besides the broad features centred at ca. 3400 cm^{-1} and 3240 cm^{-1} due to hydrogen-bonded hydroxyl groups, bands at 3092, 3069, 3037, 2963, 2941, 2885 and 2801 cm^{-1} appear upon contact of BA and water with the catalyst. As shown in Fig. 7, the bands in the 3100-2880 cm^{-1} range match the C-H stretching bands of BA. However, the band at 2801 cm^{-1}

cannot be ascribed to this species. A plausible assignment for this low frequency band would be the C-H stretching mode of an aldehyde group, what would be in agreement with an assignment to the C=O stretching of an aldehyde group for the band centred at 1705 cm^{-1}. Moreover, the bands at 1602 and 1584 cm^{-1} would agree with the presence of benzaldehyde [7]. As benzaldehyde is not expected to be formed upon adsorption at room temperature of BA on a hydroxylated titania surface, analysis of the benzyl alcohol purity was performed by HPLC. It was confirmed the presence of traces of benzaldehyde, which explains the origin of the corresponding signals in the infrared spectra. It is worthy to note that, even though the amount of adsorbed BA is similar on both titania, infrared bands due to adsorbed benzaldehyde are detected only in Degussa P25. This reveals a quite dissimilar ability of both titania samples to adsorb benzaldehyde, which is strongly retained on the Degussa P25 surface but hardly hold by HP0.5. This feature should be taken into account to explain the higher selectivity to partial oxidation of HP0.5 with respect to Degussa P25.

3.2.3. Influence of irradiation on HP0.5

After exposure to the water and BA-saturated air atmosphere for around 1 h in the dark, HP0.5 sample was irradiated, which led to the decrease in intensity of the bands derived from the alcohol adsorption together with the further enhancement of the band at 1640 cm^{-1}, and the appearance of new overlapped bands in the 1500-1400 cm^{-1} range and at ca. 1275 cm^{-1} (see Fig. 8). It should be stressed that the intensity of the δ(HOH) vibration band of adsorbed water continuously increased during irradiation but this growth stopped as soon as the lamp was switched off. This result indicates either that irradiation promotes an effective photoadsorption of water on the HP0.5 surface or that water is formed as a product of the photocatalytic degradation of the aromatic alcohol. Nevertheless, the steep increase of the band suggests that the photoadsorption phenomenon is the predominant one, as the increase of water vapour pressure from the photoreaction cannot be so fast.

The intensity and broadness of the band centred at 1640 cm^{-1} hinders the detection of other oxidation products that might be formed during irradiation such as benzaldehyde or benzoic acid, as it overlaps the carbonyl stretching region. On the other side, bands in the 1400 to 1500 cm^{-1} range and the band at 1275 cm^{-1} cannot be unequivocally assigned to specific species, but according to their wavenumber values they might be indicative of the formation of dicarboxylic

acids following the breakage of the aromatic structure. For instance, values of 1271, 1424, 1686 and 1711 cm^{-1} have been previously reported for oxalate adsorbed on TiO_2 [8]. In the same study, absorption maxima centred at 1275, 1352, 1430 and 1597 cm^{-1} were found in the infrared spectra of malonic acid adsorbed on TiO_2.

3.2.4. Influence of irradiation on commercial TiO_2

In the case of Degussa P25 sample, irradiation also produces a remarkable decrease in intensity of the bands associated to adsorbed BA (see Fig. 9). However, in contrast with HP0.5 sample, the resulting spectra show a complexity of features, whose intensity increases with the irradiation time. Besides the water bending band at 1645 cm^{-1}, the most prominent bands are peaked at 1711, 1686, 1603, 1530, 1496, 1451, 1415, 1403 (sh), 1274 and 1246 cm^{-1}. The assignment given to the bands in accordance to previous studies points out to the formation of benzaldehyde and benzoic acid as main oxidation products adsorbed on the Degussa P25 surface. The band centred at 1711 cm^{-1} can be ascribed to the C=O stretching vibration of the carbonyl group of benzaldehyde [9] whereas the bands at 1603, 1530, 1496, 1451, 1415 and 1403 cm^{-1} would be indicative of the adsorption of benzoic acid as benzoate [10, 11]. Johnson et al. [10] observed in the IR spectrum of a dried TiO_2-benzoic acid aqueous dispersion features centred at 1602 and 1451 cm^{-1}, assigned to the aromatic ring C=C vibrations, a strong band at 1415 cm^{-1} assigned to the COO^- symmetric stretching vibration and a broad band centred at 1538 cm^{-1}, attributed to the COO^- asymmetric vibration. Upon adsorption of benzoic acid on TiO_2, Finnie et al. [11] observed bands at 1535 and 1505 cm^{-1} that were assigned to the $\nu_{as}(COO)$ mode and bands at 1418 and 1405 cm^{-1}, ascribed to the $\nu_s(COO)$ vibration. Splitting of the bands was ascribed to the presence of two different coordination sites on the titania surface. In both studies, the difference between the frequencies of asymmetric and symmetric COO^- group vibrations ($\Delta\nu = \nu_{as} - \nu_s$) was observed to be higher than that of the benzoate anion, which led to the conclusion that benzoic acid was adsorbed on TiO_2 as a bidentate complex, either chelating or bridging. On this basis, in the present study the bands centred at 1603 and 1451 cm^{-1} are assigned to skeletal vibrations of the aromatic ring in adsorbed benzoic acid, whereas bands centred at 1530 and 1496 cm^{-1} are ascribed to COO asymmetric stretching vibration and the bands at 1415 and 1403 cm^{-1} to symmetric stretching. Accordingly, the largest value for the difference between the frequencies of asymmetric and symmetric COO^- group stretching vibrations would be $\Delta\nu$ = 1530-1415 = 127

cm^{-1}, value which is in agreement with a bidentate chelate or bridging coordination of benzoate on the titania surface [10, 12]. As for the band centred at 1686 cm^{-1}, it might be ascribed to the C=O stretching vibration of undissociated benzoic acid [13] which could be attached to the TiO_2 surface through either unidentate coordination or hydrogen bonding. Finally, the bands centred at 1274 and 1246 cm^{-1} must be indicative of further oxidized compounds, most likely oxalate according to the wavenumber values reported for these species [8]. In fact, it has been previously shown that oxalate hardly desorbs from the Degussa P25 surface [14] so it might be expected on the titania surface if formed during the mineralization of the aromatic alcohol.

3.2.5. Influence of ethanol co-adsorption on concentration of adsorbed species

Aiming at giving likely explanations on the influence of aliphatic alcohols on selectivity of BA oxidation [1], experiments were performed exposing samples to an atmosphere of synthetic air saturated with BA, ethanol and water to obtain further information on the effect of ethanol co-adsorption on the interaction of BA with titania surfaces. The experiments were carried out by exposing the catalyst for 10 min. to BA and water and then ethanol was introduced in the cell. Figure 10 shows ATR-FTIR spectra recorded during the adsorption experiment. For HP0.5 and Degussa P25 catalysts, upon ethanol admission in the cell, bands centred at 1480, 1450, 1380, 1326, 1275, 1088 and 1046 cm^{-1} appear in the spectra. These features are identical to the absorptions observed in the spectrum of neat ethanol (spectra not shown) thus indicating that ethanol is adsorbed on the catalyst surface mostly as molecular species. It is worth to note that for HP0.5 the adsorption of ethanol decreased the amount of adsorbed molecular water as indicated by the much lower intensity of the δ(HOH) vibration band compared to the spectra shown in Fig. 5. Moreover, this band shifted toward higher wavenumber values (1654 cm^{-1}) in both titania surfaces, thus indicating an interaction between adsorbed water and ethanol species most likely through hydrogen bonding. Similar effect was observed upon ethanol adsorption in the absence of BA.

From the concentration profiles reported in Fig. 6 it may be noted that the presence of ethanol has different effects on HP0.5 and Degussa P25. For both catalysts the amount of BA adsorbed on titania surfaces diminishes to a great extent as ethanol is introduced in the cell. Nevertheless, after 30 min of contact with ethanol vapour, weak bands corresponding to adsorbed benzyl alcohol at 1497 and 1208 cm^{-1} could still be clearly observed in the spectra of both

samples (see Fig. 10). Exposure to ethanol vapour also produced a significant decrease of the amount of adsorbed water in both samples. However, after the initial sharp decrease, the amount of water adsorbed on Degussa P25 slowly increased with time, while on HP0.5 sample it reached a nearly constant level, which indicates that ethanol competes more strongly with water for adsorption on HP0.5 sample than on the commercial titania.

3.2.6. Influence of ethanol co-adsorption on photo-oxidation products

Subsequent irradiation of HP0.5 sample results in the appearance of broad overlapping bands at ca. 1565 and 1522 cm^{-1}, that can be assigned to carboxylate species derived from ethanol photo-oxidation [15] and the growing in of bands centred at 1407 and 1350 cm^{-1} (see Fig. 11). Note particularly that, in contrast with results obtained in the absence of ethanol, the carbonyl stretching region is not hidden by the δ(HOH) band due to the lower adsorbed water content that induces the co-adsorption of ethanol. Therefore, it can be now clearly observed that no characteristic bands of benzaldehyde are formed.

In the case of Degussa P25, UV irradiation gives rise to a large increase of the spectra baseline at wavenumbers below 2000 cm^{-1} that peak at ca. 900 cm^{-1}. This phenomenon was reproducible and was observed only when ethanol was adsorbed on Degussa P25, either in the presence or absence of co-adsorbed BA. This UV-induced infrared absorption has been already reported for dry Degussa P25 and it has been attributed to excitation of shallow trap electrons to the conduction band [16]. UV light also produces the development of bands centred at 1710, 1685, 1650, 1602, 1540, 1450, 1414 and 1270 cm^{-1} indicative of the presence on the Degussa P25 surface of products derived from the oxidation of both alcohols. The finding that the bands of BA oxidation products appear also in the presence of ethanol seems to indicate that ethanol does not affect the BA oxidation pathways but it only decreases BA concentration on catalyst surface.

4. CONCLUSIONS

The photoelectrochemical characterization of HP catalysts clearly indicates that the semiconducting properties of HP0.5, HP2, HP4 and HP6 did not appreciably vary with the preparation procedure contrarily to sample HP8. The different photoactivities and selectivities

exhibited by the photocatalysts could arise hence more from different properties of their surfaces rather than from semiconducting ones.

From the ATR-FTIR analysis, it can be concluded that two main differences between HP0.5 and Degussa P25 surfaces exist. On one hand, their dissimilar hydrophilicity is relevant. A much higher amount of molecular water is indeed present on the former sample in comparison to the latter. On the other hand, the ability in adsorbing the organic compounds deriving from BA photocatalytic oxidation is quite lower for the home prepared catalyst as compared to the commercial one.

On this basis, the highest selectivity of HP0.5 sample towards BA partial oxidation can be ascribed to its low affinity for benzaldehyde adsorption, on one hand, and to the lowest mineralization promoted, on the other hand. It can be postulated that the higher hydrophilicity of HP0.5 sample compared to Degussa P25 plays an important role in connection with the latter effect, as the high coverage of the HP0.5 surface by water molecules might result in a competition for adsorption sites.

Bearing in mind the difficulty of stating clear correlations between photoreactivity and catalysts features, the following considerations may be drawn. The photoactivity results [1] obtained with HP0.5 catalyst show a low oxidation rate of benzyl alcohol but a high selectivity to benzaldehyde. The present study shows that the surface of HP0.5 catalyst is rich in molecularly adsorbed water, which is able to displace BA molecules in the dark. Under irradiation, water displaces benzyl alcohol more effectively and determines a very low coverage of alcohol molecules on HP surface. It is likely that this low coverage is responsible for the low oxidation rate of benzyl alcohol. On the other hand, the high water content might account for the high selectivity to benzaldehyde, assuming that water compete with BA molecules for the adsorption on mineralization sites. The presence of ethanol lowers the BA amount on HP surface, thus determining a strong decrease of the overall alcohol oxidation rate. Molecularly adsorbed water is also partly displaced by ethanol but the selectivity to benzaldehyde is increased. One plausible explanation is that ethanol is predominantly adsorbed on mineralization sites.

For Degussa P25 the reactivity results indicate that the mineralization pathway predominates over the partial oxidizing one. As compared to HP0.5, this catalyst shows a higher coverage of benzyl alcohol and smaller water content so that the ratio between water and benzyl alcohol is low and, therefore, it is likely that mineralization sites are not preferentially occupied

by water molecules. The addition of ethanol determines a strong decrease of benzyl alcohol coverage while the water content is poorly modified. For this catalyst neither the benzyl alcohol oxidation rate nor the selectivity to benzaldehyde is affected by ethanol so that it may be hypothesised that under irradiation the benzyl alcohol and water coverages on P25 surface remain unaltered and therefore also the partial oxidation and mineralization pathways.

ACKNOWLEDGEMENTS

Eng. Dr. Fabio D'Agostino is gratefully acknowledged for the execution of TG measurements.

REFERENCES

1. V. Augugliaro, H. Kisch, V. Loddo, M. J. López-Muñoz, C. Márquez-Álvarez, G. Palmisano, L. Palmisano, F. Parrino, S. Yurdakal, Appl. Catal. A: Gen. (2008) (submitted).
2. G. Palmisano, S. Yurdakal, V. Augugliaro, V. Loddo, L. Palmisano, Adv. Synth. Catal. 349 (2007) 964.
3. G. Kortüm, Reflectance Spectroscopy: Principles, Methods, Applications, Springer-Verlag, New York, 1969.
4. A. M. Roy, G. C. De, N. Sasmal, S. S. Bhattacharyya, Int. J. Hydrogen Energy 20 (1995) 627.
5. J. Tauc, R. Grigorovici, A. Vanuc, Phys. Stat. Sol. 15 (1996) 627.
6. G. Redmond, D. Fitzmaurice, J. Phys. Chem. 97 (1993) 1426.
7. C. Keresszegi, D. Ferri, T. Mallat, A. J. Baiker, J. Phys. Chem. B 109 (2005) 958.
8. K. D. Dobson, A. J. McQillan, Spectrochim. Acta, Part A 55 (1999) 1395.
9. H. Lampert, W. Mikenda, A. Karpfen, J. Phys. Chem. A 101 (1997) 2254.
10. A. M. Johnson, S. Trakhtenberg, A. S. Cannon, J. C. Warner, J. Phys. Chem. A 111 (2007) 8139.
11. K. S. Finnie, J. R. Bartlett, J. L. Woolfrey, Langmuir 14 (1998) 2744.
12. S. Tunesi, M. Anderson, Langmuir 8 (1992) 487.
13. M. Boczar, K. Szczeponek, M. J. Wójcik, C. Paluszkiewicz, J. Mol. Structure 700 (2004) 39.
14. I. Dolamic, T. Bürgi, J. Phys. Chem. B 110 (2006) 14898.
15. D. V. Kozlov, E. A. Paukshtis, E. N. Savinov, Appl. Catal. B: Environ. 24 (2000) L7.
16. D. S. Warren, A. J. McQuillan, J. Phys. Chem. B 108 (2004) 19373.

CAPTIONS

Figure 1. Transformed diffuse reflectance spectra of (a) HP0.5 and (b) HP8.

Figure 2. Thermogravimetric (dotted lines) and time derivative (continuous lines) curves in air of HP0.5 (▬) and Degussa P25 (▬).

Figure 3. Variation of photovoltage with pH value. 50 mg of catalyst with 10 mg of methyl viologen dichloride are suspended in 50 mL of 0.1 M KNO_3 aqueous solution at room temperature. Pt, working electrode and Ag/AgCl, reference electrodes.

Figure 4. Variation of photovoltage with pH value for HP0.5 catalyst in the presence (a) and in the absence (b) of ethanol. 50 mg of catalyst with 10 mg of methyl viologen dichloride are suspended in 50 mL of 0.1 M KNO_3 aqueous solution at room temperature. Pt, working electrode and Ag/AgCl, reference electrodes. For (b) case 5 ml of ethanol have been added to suspension.

Figure 5. Time-resolved ATR-FTIR spectra of HP0.5 thin film recorded during adsorption of water and benzyl alcohol (BA) vapours at room temperature. The arrows indicate the time when each adsorbate was introduced in the cell. The spectrum of neat benzyl alcohol (*) multiplied by a factor 0.01 has been included for comparison.

Figure 6. Time evolution of the integrated absorbance of IR bands at 1640 cm^{-1} (water), 1208 cm^{-1} (benzyl alcohol: BA) and 2975 cm^{-1} (ethanol: EA) determined from ATR-FTIR spectra recorded during adsorption of water and benzyl alcohol (top) and water, benzyl alcohol and ethanol (bottom) on HP0.5 (left) and Degussa P25 (right) samples. Zero time corresponds to introduction of BA into the cell. EA was introduced in the cell 10 min. after BA.

Figure 7. Time-resolved ATR-FTIR spectra of Degussa P25 thin film recorded during adsorption of water and benzyl alcohol (BA) vapours at room temperature. The arrows indicate the time

when each adsorbate was introduced in the cell. The spectrum of neat benzyl alcohol (*) multiplied by a factor 0.01 has been included for comparison.

Figure 8. Time-resolved ATR-FTIR spectra recorded during irradiation of HP0.5 thin film in an atmosphere of synthetic air saturated with water and benzyl alcohol. The arrows indicate the time when UV lamp was switched on (it took around 2 min to reach full power) and off.

Figure 9. Time-resolved ATR-FTIR spectra recorded during irradiation of Degussa P25 thin film in an atmosphere of synthetic air saturated with water and benzyl alcohol. The arrows indicate the time when UV lamp was switched on (it took around 2 min to reach full power).

Figure 10. Time-resolved ATR-FTIR spectra of Degussa P25 (left) and HP0.5 (right) thin films recorded during adsorption of water, benzyl alcohol (BA) and ethanol (EA) vapours at room temperature. The arrows indicate the time when each adsorbate was introduced in the cell.

Figure 11. Time-resolved ATR-FTIR spectra recorded during irradiation of Degussa P25 (left) and HP0.5 (right) thin film in an atmosphere of synthetic air saturated with water, benzyl alcohol and ethanol. The arrows indicate the time when UV lamp was switched on (it took around 2 min to reach full power) and off. Spectra of Degussa P25 sample recorded after switching off the lamp have been shifted upwards by 0.12 absorbance units for clarity.

Table 1. Photoelectrochemical properties of catalysts.

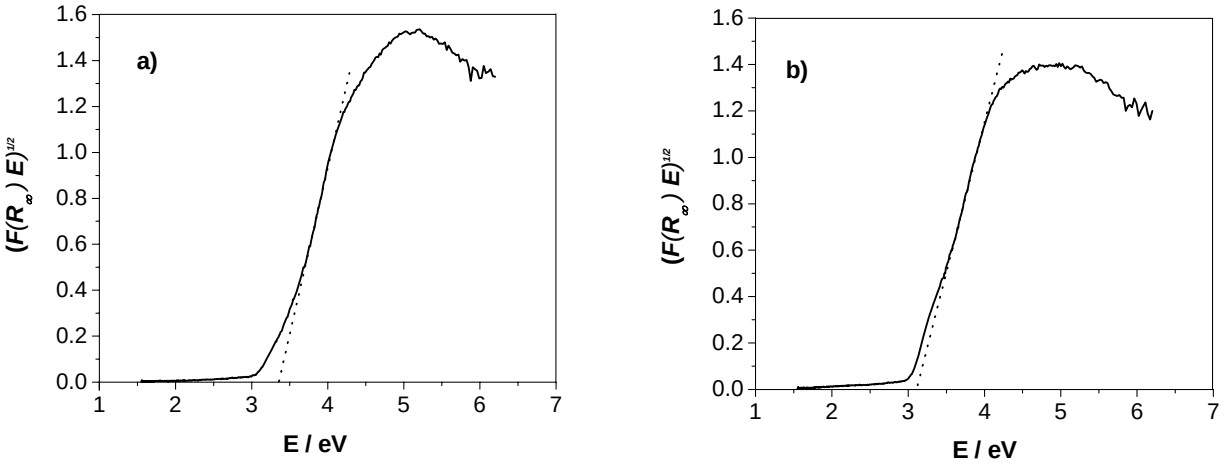

Figure 1.

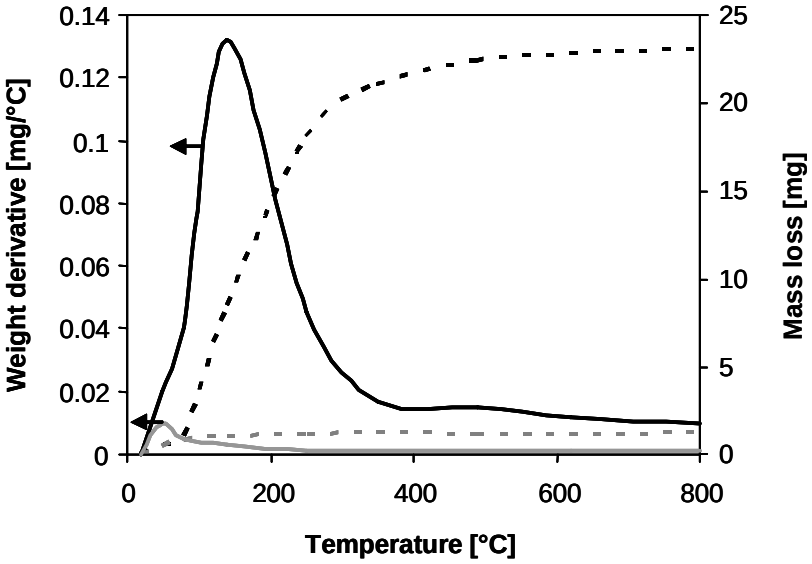
0.14
0.12
0.1
0.08
0.06
0.04
0.02
0
25
20
15
10
5
0
0
200
400
600
800
Weight derivative [mg/°C]
Mass loss [mg]
Temperature [°C]

Figure 2

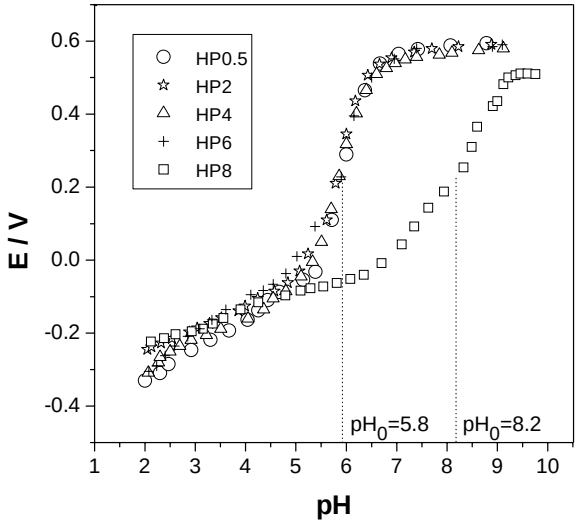
HP0.5
HP2
HP4
HP6
HP8
E / V
pH
pH0=5.8
pH0=8.2
0.6
0.4
0.2
0.0
-0.2
-0.4
1
2
3
4
5
6
7
8
9
10

Figure 3.

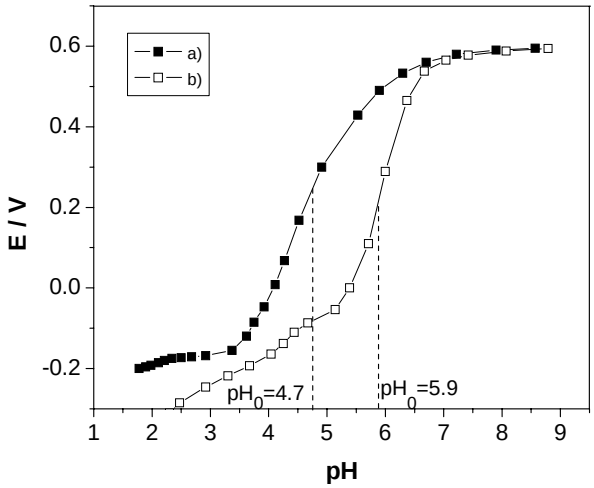

Figure 4.

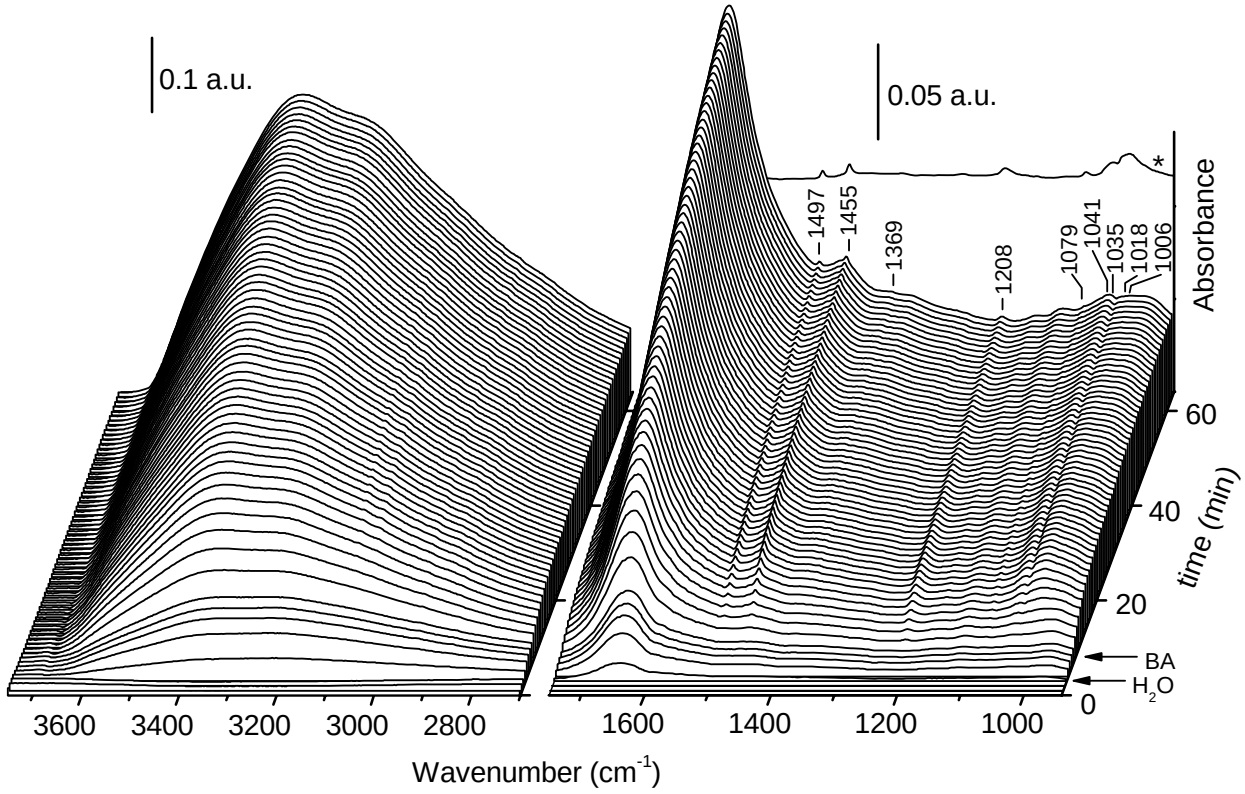
0.1 a.u.
0.05 a.u.
1497
1455
1369
1208
1079
1041
1035
1018
1006
*
Absorbance
60
40
20
0
time (min)
BA
H2O
3600
3400
3200
3000
2800
1600
1400
1200
1000
Wavenumber (cm-1)

Figure 5.

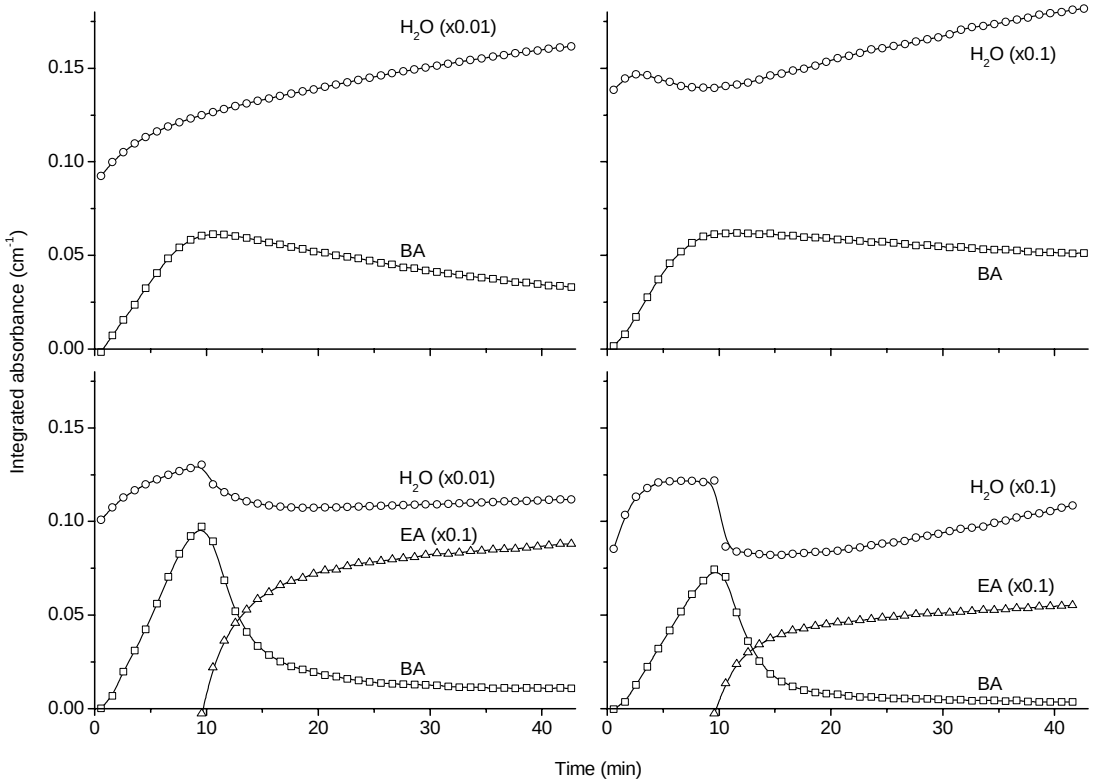
H2O (x0.01)
H2O (x0.1)
BA
EA (x0.1)
Integrated absorbance (cm-1)
Time (min)
0.00
0.05
0.10
0.15
0
10
20
30
40

Figure 6.

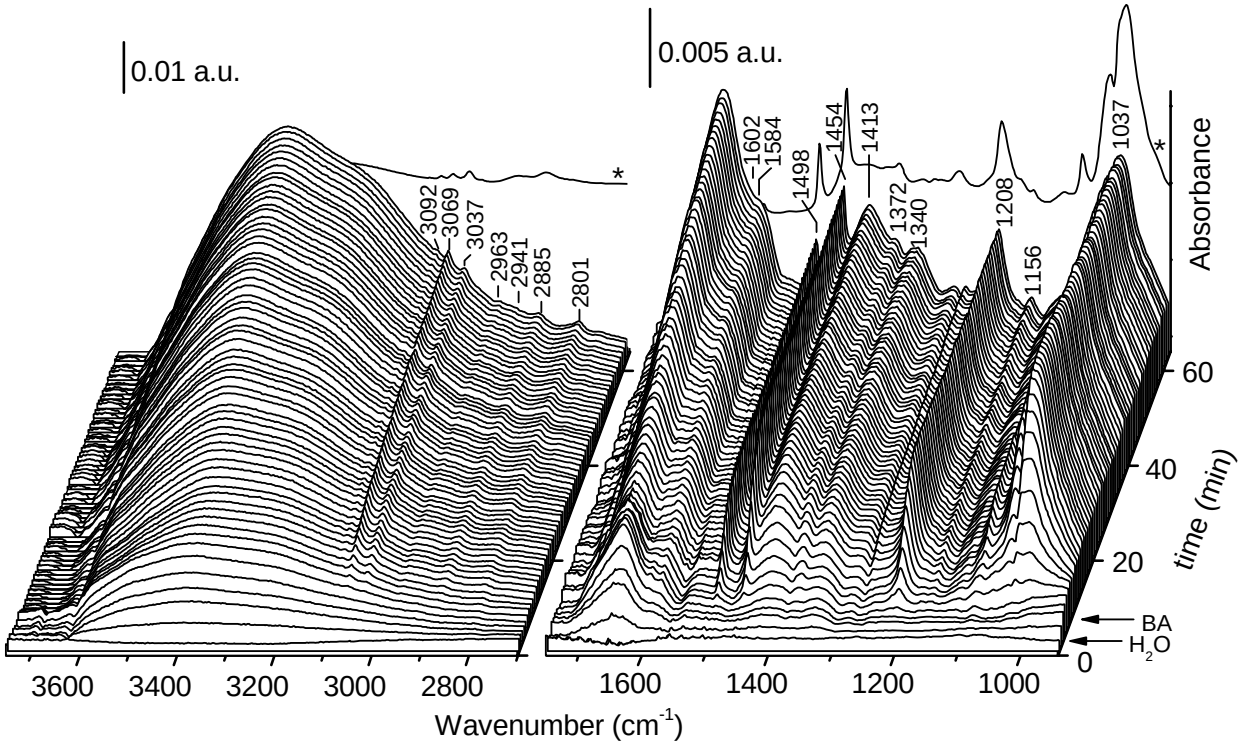
0.01 a.u.
0.005 a.u.
3092
3069
3037
2963
2941
2885
2801
1602
1584
1498
1454
1413
1372
1340
1208
1156
1037
*
Absorbance
time (min)
60
40
20
0
BA
H2O
3600
3400
3200
3000
2800
1600
1400
1200
1000
Wavenumber (cm-1)

Figure 7.

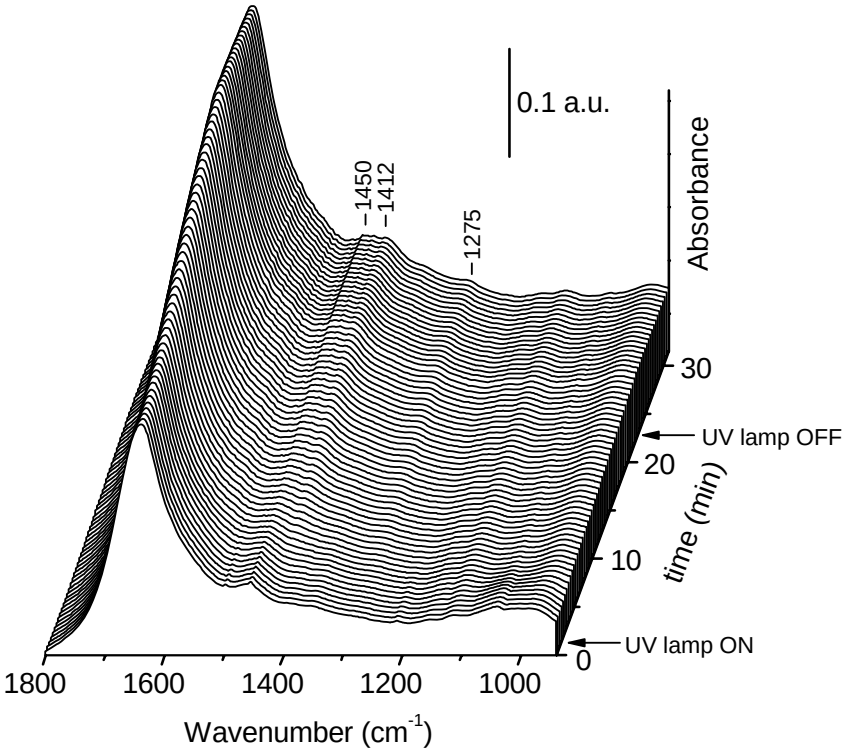
0.1 a.u.
1450
1412
1275
Absorbance
30
20
10
0
time (min)
UV lamp OFF
UV lamp ON
1800
1600
1400
1200
1000
Wavenumber (cm-1)

Figure 8.

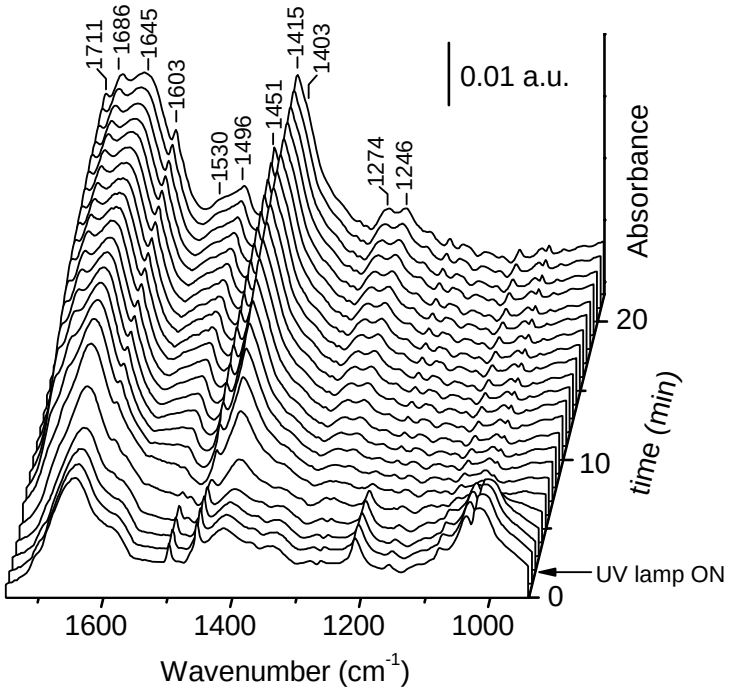
1711
1686
1645
1603
1530
1496
1451
1415
1403
1274
1246
0.01 a.u.
Absorbance
20
10
time (min)
UV lamp ON
0
1600
1400
1200
1000
Wavenumber (cm-1)

Figure 9.

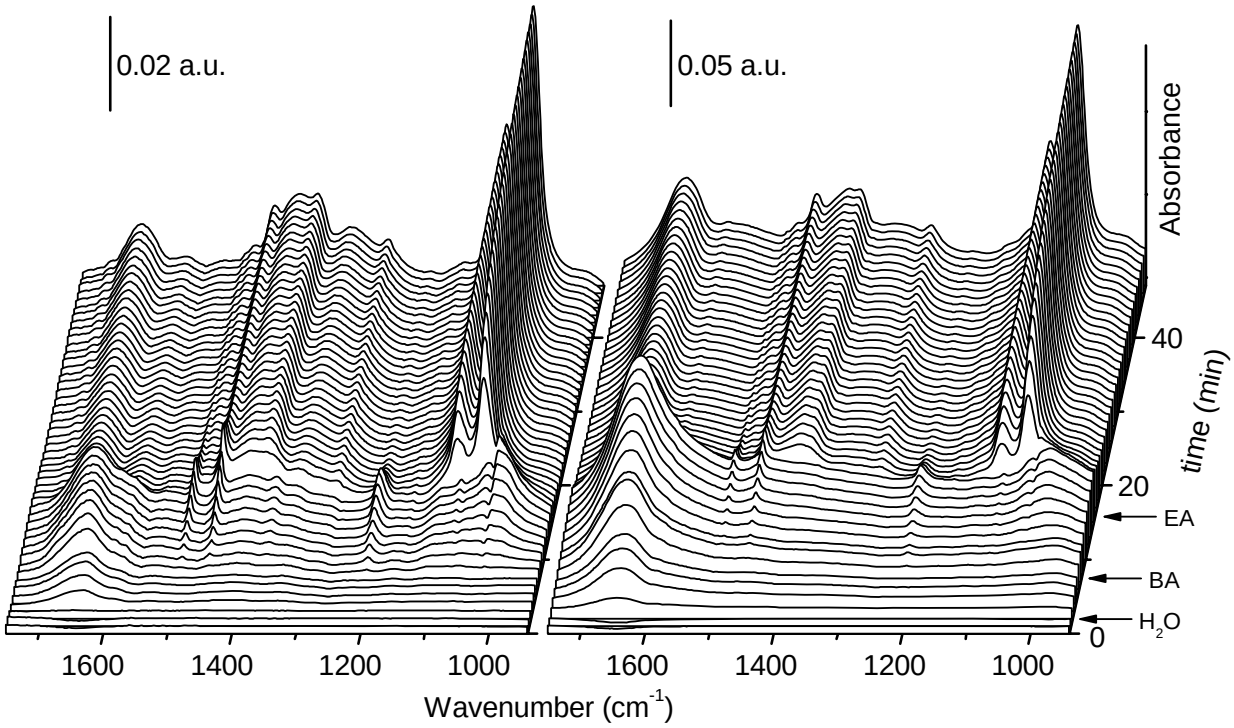
0.02 a.u.
0.05 a.u.
Absorbance
time (min)
40
20
0
EA
BA
H2O
1600
1400
1200
1000
1600
1400
1200
1000
Wavenumber (cm-1)

Figure 10.

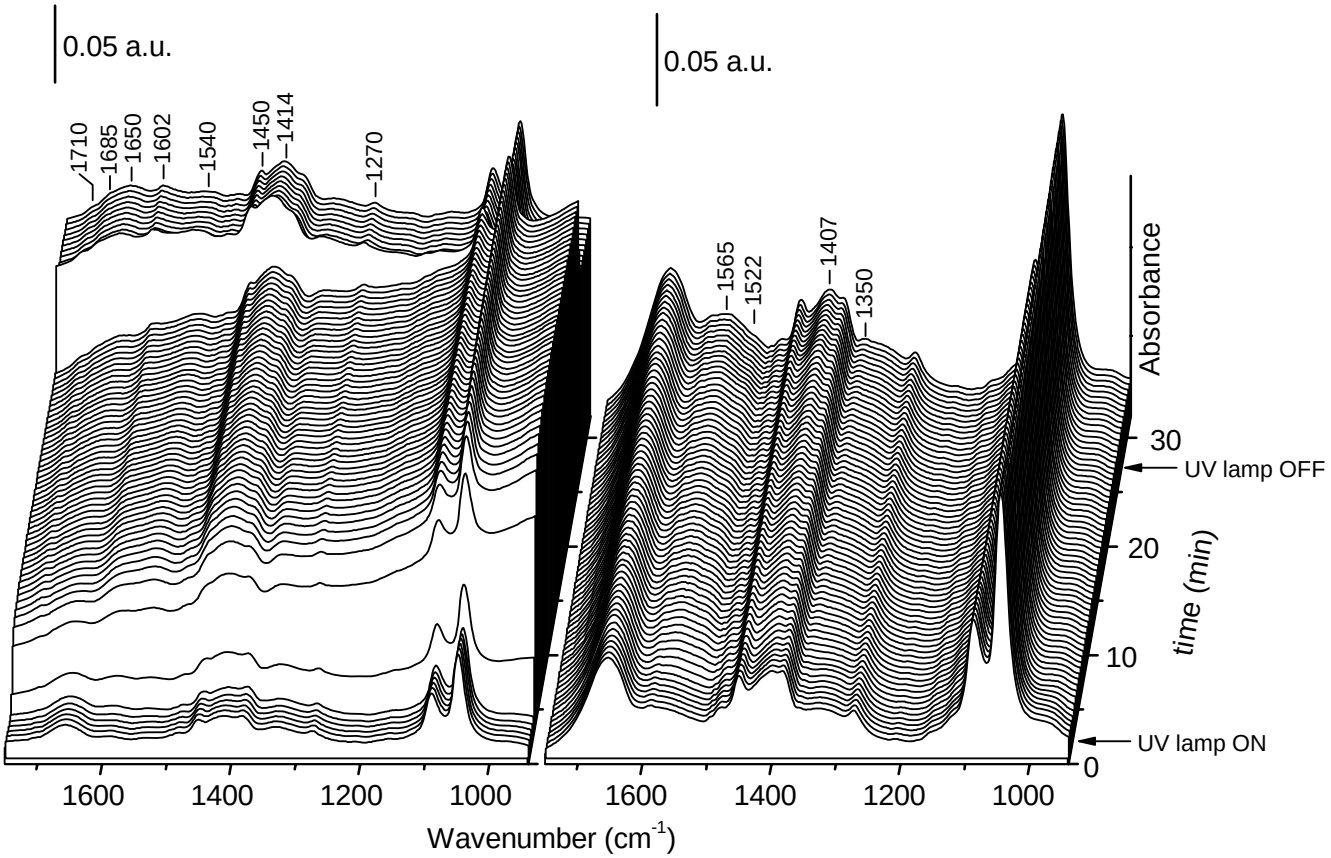
0.05 a.u.
0.05 a.u.
1710
1685
1650
1602
1540
1450
1414
1270
1565
1522
1407
1350
Absorbance
30
20
10
0
time (min)
UV lamp OFF
UV lamp ON
1600
1400
1200
1000
1600
1400
1200
1000
Wavenumber (cm-1)

Figure 11.

Table 1.

Catalyst	Band gap [eV]	E_{fb} (pH=7) [V]	VB edge [V]
Degussa P25	3.26	– 0.55 – 0.64[a]	2.71
Merck	3.22	– 0.43	2.79
HP0.5	3.36	– 0.52 – 0.58[a]	2.84
HP2	3.36	– 0.52	2.84
HP4	3.36	– 0.52	2.84
HP6	3.26	– 0.52	2.74
HP8	3.11	– 0.37	2.74

[a] values obtained in the presence of ethanol